Addressing Uncertainty in Rock Properties Through Geostatistical Simulation

Sean A. McKenna[1], Marc V. Cromer[2], Christopher A. Rautman[1] and William P. Zelinski[2]

Abstract

Fracture and matrix properties in a sequence of unsaturated, welded tuffs at Yucca Mountain, Nevada, are modeled in two-dimensional cross-sections through geostatistical simulation. In the absence of large amounts of sample data, an interpretive, deterministic, stratigraphic model is coupled with a gaussian simulation algorithm to constrain realizations of both matrix porosity and fracture frequency. Use of the deterministic, stratigraphic model imposes scientific judgment, in the form of a conceptual geologic model, onto the property realizations. Linear coregionalization and a regression relationship between matrix porosity and matrix hydraulic conductivity are used to generate realizations of matrix hydraulic conductivity. Fracture-frequency simulations conditioned on the stratigraphic model represent one class of fractures (cooling fractures) in the conceptual model of the geology. A second class of fractures (tectonic fractures) is conceptualized as fractures that cut across strata vertically and includes discrete features such as fault zones. Indicator geostatistical simulation provides locations of this second class of fractures. The indicator realizations are combined with the realizations of fracture spacing to create realizations of fracture frequency that are a combination of both classes of fractures. Evaluations of the resulting realizations include comparing vertical profiles of rock properties within the model to those observed in boreholes and checking intra-unit property distributions against collected data. Geostatistical simulation provides an efficient means of addressing spatial uncertainty in dual continuum rock properties.

INTRODUCTION

A suitability criterion for siting a national, high level, nuclear waste repository is the requirement that there be a small probability of radionuclides migrating to the accessible environment in less than 1000 years. Yucca Mountain, Nevada is currently under consideration by the U.S. Department of Energy as a

[1] Sandia National Laboratories, Geohydrology Department, PO Box 5800, Albuquerque, NM 87185-1324.
[2] Spectra Research Institute, 1613 University Blvd., NE, Albuquerque, NM, 87102

This work was supported by the United States Department of Energy under Contract DE-AC04-94AL85000.

DISCLAIMER

potential site for such a repository. In order to evaluate Yucca Mountain in terms of the 1000 year criterion, a series of groundwater travel time (GWTT) calculations have been conducted over the past three years. Given that the advective travel times will be analyzed probabilistically to determine whether or not a potential site passes the stated criterion, a Monte-Carlo approach to estimating GWTT has been employed.

Rock-property data collected at Yucca Mountain are sparse; however, conceptual models of the relationship between rock properties and geology at Yucca Mountain have been documented by extensive geologic studies in the area (e.g., Rautman and Flint, 1992; Rautman et al., 1993), sampling of rock properties along outcrop transects (e.g., Istok, et al., 1994, Flint, et al., 1995), and analysis of available data in boreholes (e.g., Engstrom and Rautman, written communication[3]). These efforts toward determining the relationship between framework geology and rock properties have provided four significant conceptual models of the geology that must be represented in the GWTT calculations: (1) the nature of the stratigraphic layering and its control on porosity; (2) the different relationships between matrix porosity and $\log_{10}$ saturated matrix hydraulic conductivity (K_{sat}) in the zeolitized and non-zeolitized portions of the mountain; (3) the relationship between fracture frequency and degree of welding; and (4) deterministic fault zones that are considered to have higher fracture frequency than the surrounding, unfaulted rock.

The goal of this paper is to demonstrate a practical means by which spatial variability of rock properties important to flow in an unsaturated domain can be tied to conceptual models of geology at the site. The technique is illustrated using stochastic rock property models generated along cross-sections used in the 1995 GWTT calculations for Yucca Mountain. Spatial variability of the properties is modeled through geostatistical simulation. These simulations are tied to the interpreted geologic framework. Special consideration is given to including the effects of zeolitization and two models of fracture formation. These simulations form the basis of the input to unsaturated zone GWTT calculations.

INTEGRATING FRAMEWORK GEOLOGY AND GEOSTATISTICAL SIMULATION

For the 1995 iteration of the GWTT calculations, rock property models were required along four cross-sections bisecting the areal extent of the proposed repository (Figure 1). The cross-sections were selected to provide a representative sampling of stratigraphy, fault conditions and infiltration rates within the area of the proposed repository. The examples discussed in this paper are drawn from modeling done on cross-section AA (Figure 1) between the water table and the topograhic surface.

[3] Engstrom, D.A. and C.A. Rautman, (in draft) Geology of the USW SD-9 Drill Hole, Yucca Mountain, Nevada, Letter Report, Sandia National Laboratories, Albuquerque, NM, 166 pp.

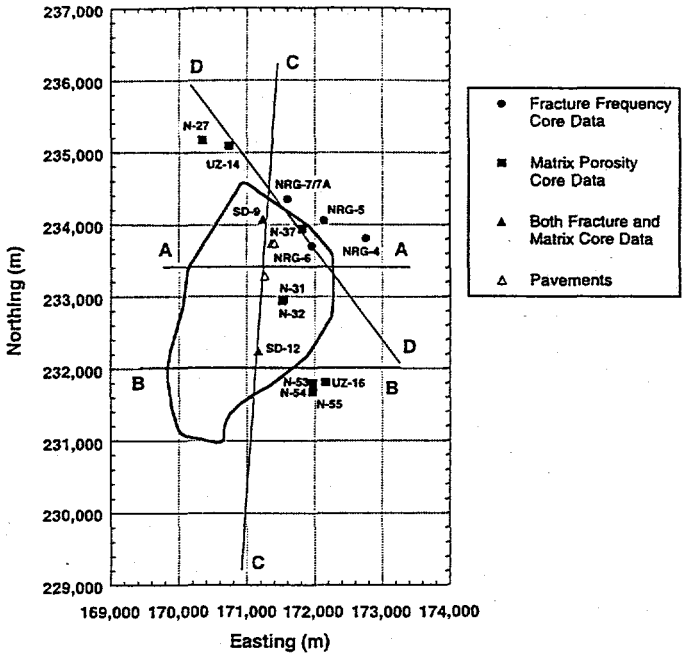

Figure 1. Map showing the locations of the four cross-sections analyzed in the 1995 GWTT calculations. The polygon defining the outline of the potential repository is also shown along with the location of conditioning data boreholes. This map uses the Nevada State Plane coordinate system (after, Altman, et al., (in press)).

The sparse amount of conditioning data at Yucca Mountain has created difficulties for geostatistical simulation of rock properties in previous studies (e.g., Rautman, 1994; Robey, 1994). Geostatistical simulation of rock properties at Yucca Mountain requires conditioning information in addition to measured property data from the available boreholes. This additional constraining information is provided by a conceptual geologic framework model of Yucca Mountain. A three-dimensional, interpretative, deterministic conceptualization of the stratigraphy at the Yucca Mountain site has been developed in a digital geologic framework model (Zelinski, written communication[4]). A total of 36 lithologic units have been entered into this digital model. The locations and geometries of these units are derived from geologic interpretation based on stratigraphic contacts observed in the available boreholes and along outcrops. For the GWTT calculations, lithologic units are combined based on similarities in porosity and geologic origin. This combination of geologic units results in nine hydrogeologic units that are used to constrain simulations of rock properties. The hydrogeologic units in the geologic framework model are shown for cross-section AA in Figure 2, and the names of the units and mean porosity and standard deviation are given in Table 1. The deterministic, geologic framework model also includes the locations and offsets of faults as mapped by the U.S. Geological Survey (Scott, 1990).

[4] Zelinski, W.P. (in draft), A Subregional Model of Lithologies, Stratigraphy and Rock Properties Encompassing the Yucca Mountain Project Conceptual Controlled Area, Yucca Mountain, Nevada, SAND Report, Sandia National Laboratories, Albuquerque, NM

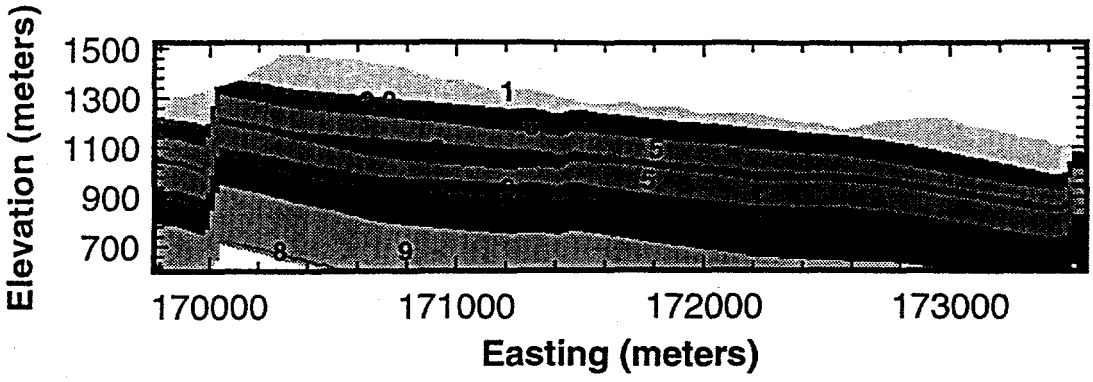

Figure 2. Deterministic interpretation of location and geometry of hydrogeologic units in the stratigraphic framework model along cross-section AA. The numbers of the units correspond to the numbers given in Table 1.

TABLE 1. Hydrogeologic unit names and identifiers with porosity and fracture frequency statistics.

Unit #	Unit Name	Mean Porosity (fraction)	Porosity std. dev. (fraction)	Mean Fracture Frequency ($\log_{10}$ 1/m)
1	Tiva Canyon	0.09	0.07	1.16
2	Paintbrush Group #1 (PTn1)	0.46	0.08	0.47
3	Paintbrush Group #2 (PTn2)	0.28	0.10	0.47
4	Vitrophyre	0.05	0.05	1.07
5	Topopah Spring Lithophysal	0.13	0.04	1.21
6	Topopah Spring Nonlithophysal	0.10	0.04	1.23
7	Calico Hills	0.23	0.07	0.35
8	Prow Pass-Bullfrog Welded	0.15	0.04	1.22
9	Prow Pass-Bullfrog Nonwelded	0.25	0.06	0.47

For the 1995 GWTT calculations, software was written that would allow direct coupling of the geostatistical simulation process with an interpretation of the geology at the site (Cromer and Rautman, in press). This software is known as the GSLIB-LYNX integration module (GLINTMOD) and it provides a link between the sequential gaussian simulation program SGSIM from the GSLIB software library (Deutsch and Journel, 1992) and the geologic framework modeling software LYNX (Lynx Geosystems, Vancouver, B.C.). The link between the two software packages allows a location being simulated in the SGSIM coordinate system to access the geologic framework model and determine the expected value of the property being simulated within the specific hydrogeologic unit. In the current version of GLINTMOD, information from the geologic framework model is used in the geostatistical simulation when the number of conditioning points found within the local simulation search neighborhood is less than a user-specified minimum. In such cases, the mean property value for the relevant hydrogeologic unit is determined from the geologic framework model and passed back to SGSIM. This mean is then used to center the conditional cdf used in the Monte Carlo simulation process (see Deutsch and Journel, 1992). The geologic framework model is called often in the early stages of the simulation when there are few previously simulated nodes and then, as the simulation domain is populated, additional points are conditioned upon previously simulated nodes.

SIMULATION OF MATRIX PROPERTIES

Matrix porosity simulations (e.g., Figure 3) are created using porosity data from boreholes shown in Figure 1 as conditioning data and the deterministic interpretation of the geology along each cross-section (e.g., Figure 2). The statistical characteristics of matrix porosity data are summarized in Table 1. Matrix porosity values are controlled by the degree of welding within each lithologic unit. A spherical variogram model with a range of 457 meters and a ten percent nugget effect is used in the matrix porosity simulations. The horizontal to vertical anisotropy of the modeled spatial correlation is 33.3:1.

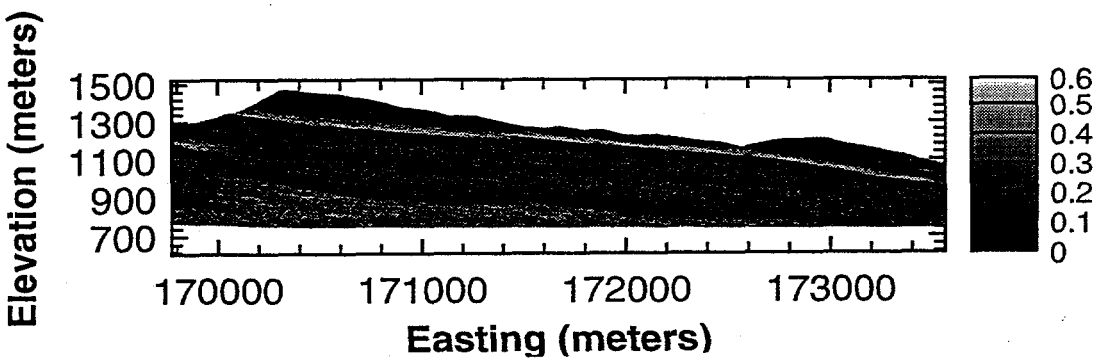

Figure 3. Example realization of matrix porosity conditioned to borehole data and the stratigraphic framework model shown in Figure 2.

Available data demonstrate a positive, linear regression relationship between matrix porosity and matrix K_{sat} (Figure 4). There are distinctly different relationships between these two properties within the zeolitized and non-zeolitized portions of the mountain (Figure 4). Both of these relationships must be retained in the resulting geostatistical simulations. At the present time, there are not enough K_{sat} data to develop the cross-covariances between porosity and K_{sat} necessary for geostatistical cosimulation as described by Gomez-Hernandez (1991) or Deutsch and Journel (1992). However, a model of linear coregionalization (Journel and Huijbregts, 1978; Desbarats,1995) can be used to simulate two correlated properties by assuming the models of spatial correlation for both properties and the cross-correlation model between the properties are the same.

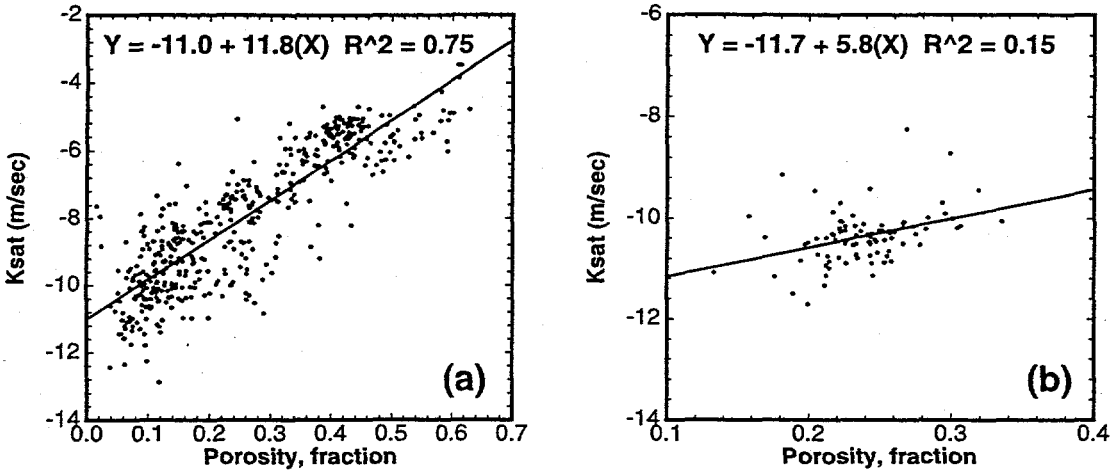

Figure 4. Regression relationship between matrix porosity and $\log_{10}$ saturated hydraulic conductivity for the non-zeolitized (A) and the zeolitized (B) portions of the mountain as derived from borehole and outcrop transect data (after Altman, et al., (in press)).

At the basis of linear coregionalization, are two constructs: the covariance matrix and the definition of the coefficient of correlation (r). The covariance matrix is given as:

$$\begin{bmatrix} C_{11} & C_{12} \\ C_{21} & C_{22} \end{bmatrix} \qquad (1)$$

where C denotes variance and the subscripts refer to two different properties Z_1 and Z_2. The final goal of the coregionalization process is to produce realizations of the two properties (e.g., matrix porosity and K_{sat}) that honor the covariance matrix derived from available data. The second construct is the relation between covariance and the coefficient of correlation between two properties:

$$r = \frac{C_{12}}{\sqrt{C_{11}C_{22}}} \qquad (2)$$

The coefficient of correlation, r, can be obtained from the regression relationship between properties, and the variances of each property are obtained from the data.

For this study, the auto and cross-covariances of the properties are defined by spherical variogram models. Spherical models have been used to model spatial correlation in previous studies at Yucca Mountain (e.g., Rautman, 1991; McKenna and Rautman, 1995). Simulations of properties Z_1 and Z_2 that fit the modeled variograms are generated by defining two new variables Y_1 and Y_2. Both of these variables have a mean equal to zero and spherical covariance functions K_1(h) and K_2(h) and they are independent of each other (i.e., K_{12}(h) = 0 for all h). Unconditional realizations of Y_1 and Y_2 are created using SGSIM (Deutsch and Journel, 1992). The original variables (Z_1,Z_2) can now be expressed as linear combinations of the new variables:

$$\begin{aligned} Z_1(x) &= a_{11}Y_1(x) + a_{12}Y_2(x) \\ Z_2(x) &= a_{21}Y_1(x) + a_{22}Y_2(x) \end{aligned} \tag{3}$$

Because the two Y variables are independent, the covariance functions of the Z's are given as:

$$\begin{aligned} C_1(h) &= a_{11}^2 K_1(h) + a_{12}^2 K_2(h) \\ C_2(h) &= a_{21}^2 K_1(h) + a_{22}^2 K_2(h) \\ C_{12}(h) &= a_{11}a_{21} K_1(h) + a_{11}a_{22} K_2(h) \end{aligned} \tag{4}$$

These equations provide a means by which two independent realizations of Y_1 and Y_2 can be combined through the coefficients of the **A** matrix to provide realizations of Z_1 and Z_2 that satisfy the covariance matrix (equation 1). The three expressions given in equation 4 are solved for the coefficients of the **A** matrix by setting one of the four coefficients equal to zero.

Linear coregionalization has been used to simulate values of K_{sat} correlated to matrix porosity within the non-zeolitized portion of the mountain. A smaller portion of the mountain has been zeolitized, and the extent of this volume is determined by review of drilling logs. K_{sat} is simulated within this volume by modeling the regression relationship between K_{sat} and porosity observed in the field (figure 4b). This relationship is modeled with the traditional linear regression equation:

$$K_{sat} = b_o + b_1(porosity) + \varepsilon \tag{5}$$

where ε are normally distributed errors about the regression line modeled in accordance with the observed coefficient of determination (Figure 4b).

SIMULATION OF FRACTURE PROPERTIES

Cooling fractures are largely a function of the lithology; more welded units exhibit higher fracture frequencies due to slower cooling. Mean values of $\log_{10}$ fracture frequency for the nine hydrogeologic units are given in Table 1. The data represent measurements of fracture frequency from approximately 550 ten-foot-long drill cores. These measurements are adjusted to account for fracture orientation relative to the vertical boreholes using the method of Scott et al. (1983). Three previously mapped rock pavements (Figure 1) (Barton, et al., 1993) were used to provide additional information on fracture frequency. Realizations of the fracture frequencies attributed to cooling processes are simulated using GLINTMOD in a similar manner to the matrix porosity simulations.

Vertical zones of relatively higher fracture frequency that cut across lithologic layering include the large scale faults that bound the potential repository block and smaller faults throughout Yucca Mountain. The locations of these zones are simulated using an indicator algorithm (SISIMPDF; Deutsch and Journel, 1992). Large scale fault zones are viewed as deterministic features and are located in the simulation domain with conditioning data (labeled fault zones in Figure 5). The smaller features are considered as randomly located features and are produced by the indicator simulation. The area within the higher frequency fracture zones is 20 percent of the total domain.

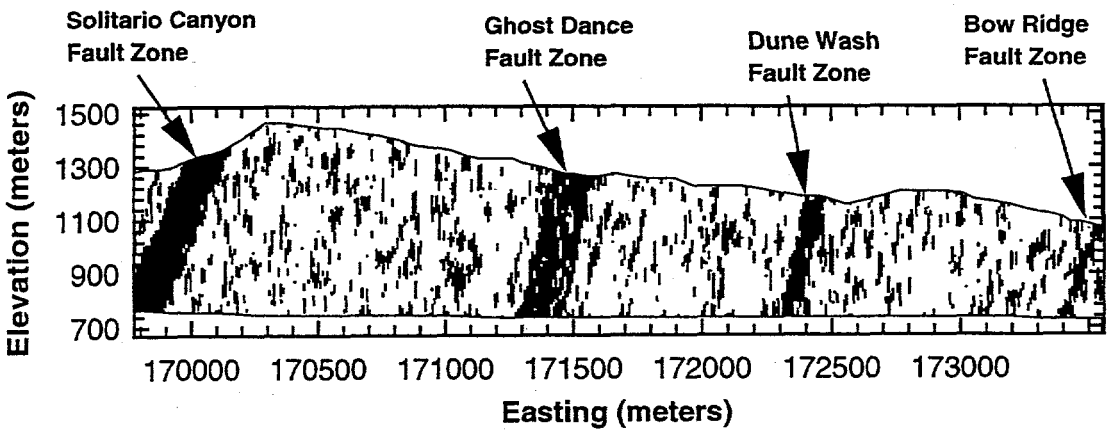

Figure 5. Realization of the high fracture frequency zones created with indicator geostatistical simulation. The mapped, deterministic fault features are labeled (after Altman, et al., in press).

Realizations created by the two fracture models are merged to create a single representation of fracture frequency that is a combination of cooling and tectonic fractures. Field studies have shown that fracture frequency within a fault zone is sharply reduced in the high porosity, nonwelded units of the Paint Brush Group and fracture frequency is also relatively low in the Calico Hills, nonwelded unit (Scott,

et al., 1983). These observations have led to the development of a relationship between porosity and the effect of tectonically induced fractures:

$$if\begin{cases}\phi < 0.40, M_{ff} = -22.5\phi + 10.0\\ \phi \geq 0.40, M_{ff} = 1.0\end{cases} \qquad (6)$$

where ϕ is matrix porosity and M_{ff} is the multiplier for fracture frequency. M_{ff} is a factor by which the cooling fracture frequency, or background frequency, is multiplied within the high frequency zones. Determination of the multiplication factor as a function of porosity forces the tectonic fractures to be more frequent in the welded zones and by terminating the slope in Equation 6 at a porosity fraction of 0.40, the nonwelded units in the Paintbrush Tuff remain essentially unaffected by tectonic fracturing (Figure 6). The model of essentially unfractured Paintbrush Tuff nonwelded units are consistent with field observations (Scott and Castellanos, 1984).

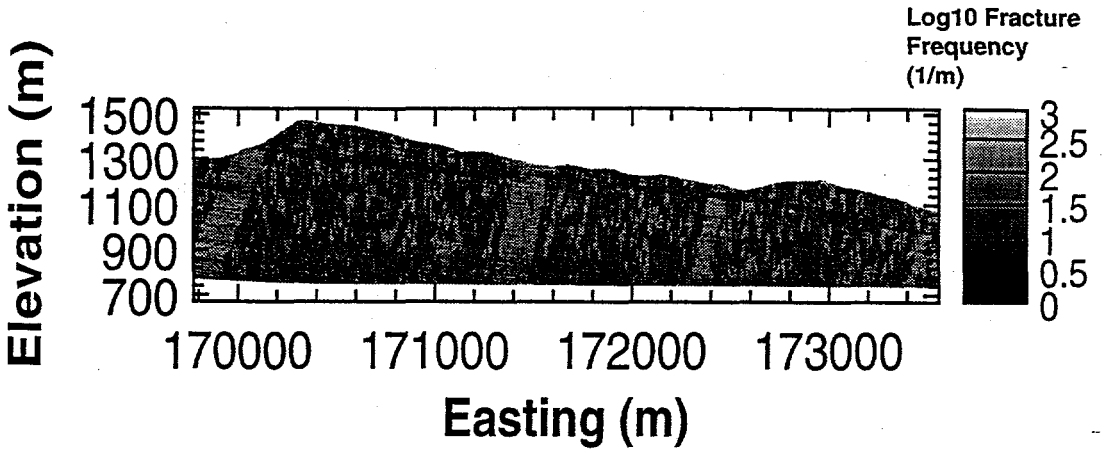

Figure 6. Example realization of $\log_{10}$ 1/m fracture frequency derived by combining realizations of cooling fractures with tectonically induced fracturing through the relationship defined in Equation 6 (after Altman, et al., in press)

EVALUATION OF ROCK PROPERTIES MODELS

In lieu of being able to compare the geostatistical simulations to exhaustive knowledge of the site, they are evaluated in a number of other ways. The conceptual model of porosity being controlled by the degree of welding is compared to borehole data. The general trend of porosity in the vertical direction has been documented from samples obtained in a number of boreholes. The porosity profile in borehole SD-9 (Figure 7a) is representative of those across the site.

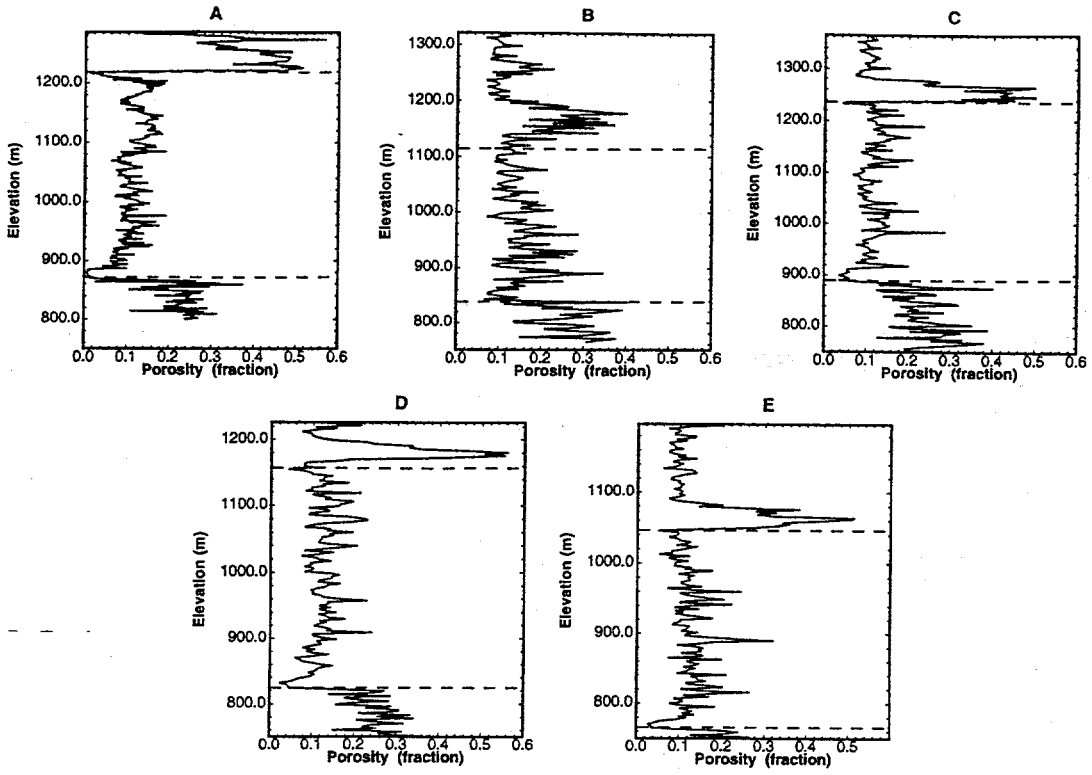

Figure 7. Comparison of porosity trends in boring SD-9 (a) with four vertical profiles taken along section AA. The profiles were extracted from the realization shown in Figure 3 at the easting coordinates: 170,000m (b), 171,000m (c), 172,000m (d), and 173,000m (e). The dashed lines are the inferred top and bottom of the Topopah Spring unit. Vitrophyre occurs at the top and bottom of the Topopah Spring (after Altman, et al., in press)

The high porosity of the PTn2 unit (above Topopah Spring) and the low porosity of the vitrophyre (Table 1) are reproduced in all profiles. A trend of slightly decreasing porosity values from top to bottom of the Topopah Spring unit is seen in SD-9 (Figure 7a) and is well defined in profiles c and d. This trend is less defined in profiles b and e. The generally random appearance of profile b in Figure 7 is due to its location within the Solitario Canyon Fault Zone. The high variability of porosity along profile b is caused by the transect sampling porosity values from unfaulted rock on both sides of the fault zone.

To determine whether or not the GLINTMOD software is able to reproduce the measured mean and variability of porosity within the hydrogeologic units, 200 data points were extracted from each hydrogeologic unit from the realization of porosity shown in Figure 3. The means and standard deviations of the extracted data are shown in Table 2. Due to the limited extent of the Prow Pass/Bullfrog welded hydrogeologic unit (Unit 8), it was not possible to extract a representative porosity

sample from this unit. The means and standard deviations of the simulated hydrogeologic units (Table 2) compare favorably with the observed statistics for each hydrogeologic unit shown in Table 1.

Table 2. Porosity means and standard deviations for hydrogeologic units extracted from a realization of section AA.

Unit #	Mean Porosity	Std. Dev. Porosity
1	0.10	0.02
2	0.41	0.08
3	0.29	0.07
4	0.06	0.01
5	0.14	0.04
6	0.11	0.02
7	0.26	0.07
8	NA	NA
9	0.26	0.08

The relationship between porosity and K_{sat} modeled through both linear coregionalization and a linear regression model is evaluated for both the zeolitized and non-zeolitized portions of the cross-section. Figure 8 shows the regression relationships for the simulated properties. The regression relationships honor the equations derived from the sample data. The simulated results for the zeolitized portion of the cross-section have a higher coefficient of determination than the measured data. This bias in the simulated results relative to the measured data is attributed to a lack of outlier points in the simulated values and an imposed gaussian distribution of errors about the regression line compared to non-gaussian errors in the field data. The regression relation from the simulated values also extends to higher porosity values than the regressed field data. This extension is an artifact of the regression modeling process within the zeolitized zone where porosity values are simulated independently of the K_{sat} values. The field data reflect an upper limit for porosity in the neighborhood of 35 percent. As seen in Figure 8b, the majority of the porosity values are below 35 percent. However, porosity values above 35 percent are simulated in the zeolitized zone and then the regression model is applied to them to determine a value of K_{sat}. It is expected that use of a cosimulation algorithm instead of linear coregionalization would correct this problem and keep the simulated results closer to the measured results.

The conceptual models of fracturing and faulting are evaluated by visual inspection of the resulting simulations. Examination of Figure 6 shows the deterministically modeled fault zones to be in the correct locations with the correct dips and widths. The randomly simulated high fracture frequency zones are of the prescribed length, orientation and frequency and the fracture frequency within the zones is sharply reduced across the nonwelded PTn2 and Calico Hills hydrogeologic units (Figure 6).

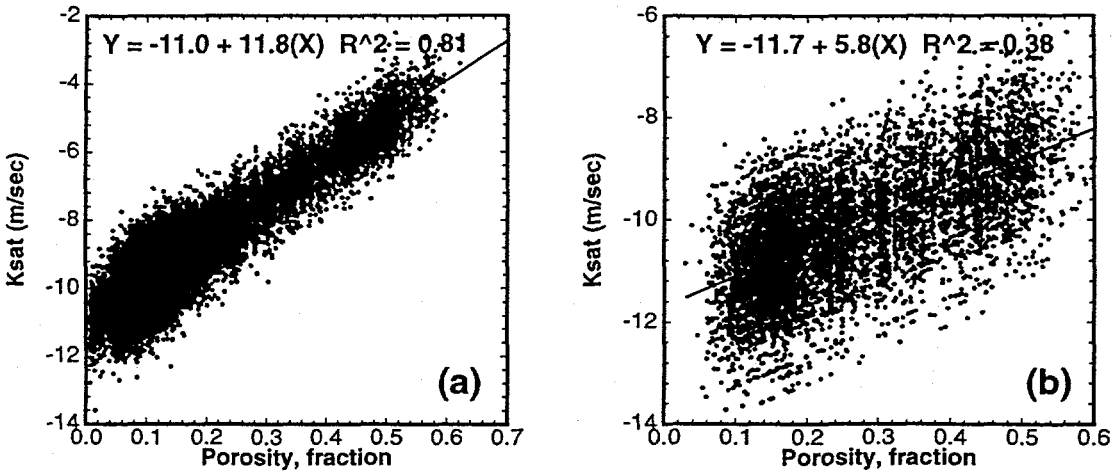

Figure 8. Regression relationship between simulated matrix porosity and $\log_{10}$ saturated hydraulic conductivity for the non-zeolitized (A) and the zeolitized portion of the mountain (B) resulting from the linear coregionalization and linear regression models applied to the matrix porosity realization shown in Figure 3 (after Altman et al., in press)

The end result of the geostatistical simulation process is to transfer the uncertainty in the spatial distribution of rock properties that results from limited sampling through a transfer function (in this case, an unsaturated flow model), to a distribution of travel times. The geostatistical simulations have been input to multiphase, dual permeability, flow simulations (Altman, et al., in press). Realizations of matrix porosity, K_{sat} and fracture frequency values were upscaled to represent flow-model elements through different averaging techniques. Porosity and fracture frequency were upscaled through arithmetic averaging and K_{sat} was upscaled through power-law averaging with a power coefficient of -0.4 as determined through numerical experiments (McKenna and Rautman, in press). The scaled values of the matrix and fracture properties at each flow-model grid block and regression relationships defined from available field data were used to define moisture characteristic curves and relative permeability curves for each flow-model grid block. Interaction between the fracture and matrix continua is modeled with Darcy's Law. The area of connection between the two continua is set to two orders of magnitude less than full geometric connection area to account for the low fracture saturations (Altman, et al., in press).

When all of the simulated rock properties are upscaled and implemented into the multiphase flow model TOUGH2 (Pruess, 1991), along with measured and inferred boundary conditions, resulting matrix saturations can be compared with measured saturations and the variability in modeled saturations between realizations can be assessed (Figure 9). The modeled saturations follow the trend of the measured saturations in borehole SD-9. Furthermore, with the exception of the

upper portion of the section, the measured matrix saturations fall within the range between minimum and maximum saturation across the realizations for each elevation (Figure 9). The discrepancy between measured and modeled saturations in the upper portion of the profile is due to modeling all infiltration as occurring in the fractures.

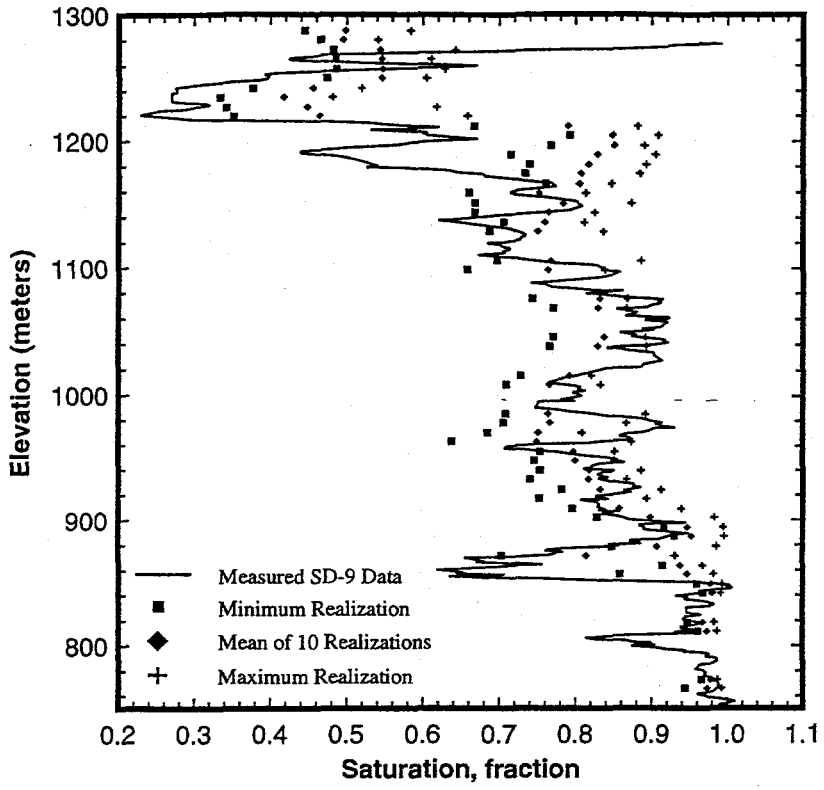

Figure 9. Comparison of matrix saturation profile in boring SD-9 (solid line) with the mean (diamonds), minimum (squares) and maximum (pluses) saturation values for the corresponding elevations resulting from flow modeling using 10 realizations of rock properties as input. The solid line representing the SD-9 data is a five point running average of the core-plug saturation measurements.

SUMMARY

In addition to conditioning rock property data, conceptual models of the geology and stratigraphy of a site can be used to guide the geostatistical simulation process. Results from the Yucca Mountain example indicate that conceptual models derived from site investigations and geologic interpretation can be readily incorporated into a stochastic modeling exercise. By coupling the simulation of porosity with a geologic framework model, the resulting realizations reflect the stratigraphic control of porosity and, on average, reproduce the geologic framework

model. Combining gaussian simulation with linear coregionalization has reproduced the regression model between porosity and K_{sat} across the model domain. A further combination of gaussian simulation, conditioned to the geologic framework model, and indicator simulation produced stochastic realizations of stratigraphically controlled fracture frequency overprinted by high fracture frequency zones resulting from tectonic activity.

In a stochastic modeling exercise, it is the random component of the process that gives the results their variability. The true amount of spatial variability is never known, but can only be estimated. Determination of whether or not the actual variability is being estimated accurately can be made by comparing measured and modeled results. In this study, the vertical profiles extracted from a simulation of porosity indicate that the modeling process is correctly representing the vertical trends of the measured porosity. Additionally, the global mean and standard deviation of porosity within hydrogeologic units matches those parameters as measured in the field. Modeled saturation profiles approximate measured saturation profiles indicating that these rock properties models, coupled with chosen hydrologic boundary conditions, reproducing the essential character of the rock mass at Yucca Mountain.

REFERENCES

Altman, S.J., B.W. Arnold, C.K. Ho, S.A. McKenna, R.W. Barnard, G.E. Barr and R.R. Eaton, (in press)Flow Calculations for Yucca Mountain Ground Water Travel Time (GWTT-95), SAND Report, Sandia National Laboratories, Albuquerque, NM.

Barton, C.C., C.E. Larsen, W.R. Page and T.M. Howard, 1993, Characterizing Fractured Rock for Fluid-Flow, Geomechanical and Paleostress Modeling: Methods and Preliminary Results for Yucca Mountain, Nevada, *USGS-OFR-93-269*, U.S. Geological Survey, Denver, CO.

Cromer, M.V. and C. A. Rautman, (in press), Use of Stratigraphic Models as Soft Information to Constrain Stochastic Modeling of Rock Properties: Development of the GSLIB-Lynx Integration Module, *SAND95-2338*, Sandia National Laboratories, Albuquerque, NM.

Desbarats, A.J., 1995, Upscaling Capillary Pressure-Saturation Curves in Heterogeneous Porous Media, *Water Resour. Res.*, 31 (2). pp. 281-288.

Deutsch, C.V. and A.G. Journel, 1992, *GSLIB: Geostatistical Software Library and User's Guide*, Oxford University Press, New York, 340 pp.

Flint, L.E., A.L. Flint and C.A. Rautman, 1995, Physical and Hydrologic Properties of Rock Outcrop Samples at Yucca Mountain, Nevada, *U.S. Geological Survey, Open File Report 95-280.*

Gomez-Hernandez, J.J., 1991, A Stochastic Approach to the Simulation of Block Conductivity Fields Conditioned upon Data Measured at a Smaller Scale, Ph.D. Dissertation, Stanford Univ., 351 pp.

Istok, J.D., C.A. Rautman, L.E. Flint and A.L. Flint, 1994, Spatial Variability of Hydrologic Properties of a Volcanic Tuff, *Ground Water*, 32 (5), pp. 751-760.

Journel, A.G. and Ch. J. Huijbregts, 1978, *Mining Geostatistics*, Academic Press, London, 600 pp.

McKenna, S.A. and C.A. Rautman, (in press), Scaling of Properties for Yucca Mountain: Literature Review and Numerical Experiements on Saturated Hydraulic Conductivity, *SAND95-2338*, Sandia National Laboratories, Albuquerque, NM.

McKenna, S.A. and C.A. Rautman, 1995, Summary Evaluation of Yucca Mountain Surface Transects with Implications for Downhole Sampling, *SAND94-2038*, Sandia National Laboratories, Albuquerque, NM, 45 pp.

Pruess, K., 1991, TOUGH2--A General Purpose Numerical Simulator for Multiphase Fluid and Heat Flow, *LBL-29400*, Lawrence Berkeley Laboratory, Berkeley, Calif.

Rautman, C.A., 1991, Estimates of Spatial Correlation in Volcanic Tuff, Yucca Mountain, Nevada, *SAND89-2270*, Sandia National Laboratories, Albuquerque, NM, 110 pp.

Rautman, C.A., 1994, Development of Stochastic Indicator Models of Lithology, Yucca Mountain, Nevada, *High-Level Radioactive Waste Management, Proceedings of the Fifth International Conference*, Las Vegas, Nevada, May 22-26, American Nuclear Society, La Grange Park, Illinois, pp. 2510-2519.

Rautman, C.A. and A.L. Flint, 1992, Deterministic Geologic Properties and Stochastic Modeling, *High-Level Radioactive Waste Management, Proceedings of the Third International Conference*, April 12-16, American Nuclear Society, La Grange Park, Illinois, pp. 1617-1624.

Rautman, C.A., J.D. Istok, A.L. Flint, L.E. Flint and M.P. Chornack, 1993, Influence of Deterministic Geologic Trends on Spatial Variability of Hydrologic Properties in Volcanic Tuff, *High-Level Radioactive Waste Management, Proceedings of the Fourth International Conference*, April 26-30, American Nuclear Society, La Grange Park, Illinois, pp. 921-929.

Robey, T.H., 1994, Development of Models for Fast Fluid Pathways Through Unsaturated Heterogeneous Porous Media, *SAND93-7109*, Sandia National Laboratories, Albuquerque, NM.

Scott, R.B., 1990, Tectonic Setting of Yucca Mountain, Southwest Nevada, Basin and Range Extensional Tectonics Near the Latitude of Las Vegas, Nevada, B.P. Wernicke (ed.), *Geological Society of America Memoir 176*, Geological Society of America, Boulder, Colorado, pp. 251-282.

Scott, R.B., R.W. Spengler, S. Diehl, A.R. Lappin and M.P. Chornack, 1983, Geologic Character of Tuffs in the Unsaturated Zone at Yucca Mountain, Southern Nevada, , in: Role of the Unsaturated Zone in Radioactive and Hazardous Waste Disposal, J.W. Mercer, P.S.C. Rao and I.W. Marine (eds.), Ann Arbor Science, Ann Arbor, Michigan, pp. 289-235.

Scott, R.B. and M. Castellanos, 1984, Stratigraphic and Structural Relations of Volcanic Rocks in Drill Holes USW GU-3 and USW G-3, Yucca Mountain, Nye County, Nevada, USGS Open File Report, 84-491, US Geological Survey, Denver, Colorado, 121 pp.